## Atomistic Simulations and Their Experimental Validations for Fe Solubility in Liquid Pb

Seoyeon Bak a, Kristof Bal b, Daniel Stein b, c, Jun Lim b, Takuji Oda a\*

aDept. of Energy Systems Engineering, Seoul Natl. Univ., 1 Gwanak-ro, Gwanak-gu, Seoul 08826, Republic of Korea
bCoolant Chemistry Research (CCR), Belgian Nuclear Research Centre (SCK CEN), Boeretang 200, 2400 Mol,
Belgium<sup>c</sup> Sustainable Materials Engineering, Vrije Universitet Brussles (VUB), Pleinlaan 2, 1050 Brussels, Belgium
\*Corresponding author: oda@snu.ac.kr

\*Keywords: heavy liquid metal, corrosion, atomistic simulations, electrochemical measurement

#### 1. Introduction

Heavy liquid metals, such as liquid lead (Pb), have been adopted as the primary coolant in lead-cooled fast reactors (LFRs) and accelerator-driven systems (ADSs). One of the main engineering challenges in these reactors is the corrosion of the structural steels, since some of the steel components, such as iron (Fe) and nickel (Ni), have high solubility in liquid Pb. SCK CEN has developed an electrochemical method for measuring solubility of metallic impurities in liquid Pb [1], in which the solubility is derived from the solubility product of the oxide, as measured by coulometric titration of oxygen (O).

Atomistic simulations have emerged as an alternative to experiments for determining various material properties. However, solubility is in general difficult to determine by atomistic simulations unless solubility is very high. In our previous study [2], we calculated the Fe solubility in liquid Pb by the brute force direct coexistence method (DCM), which had unaffordable computational costs.

In this study, we make use of the so-called semi-grand canonical Monte-Carlo (SGCMC) ensemble [3] to calculate solubility, which greatly reduces the computational cost. Taking the Fe solubility in liquid Pb as a test case, we calculate the solubility and validate the results with the electrochemical measurements carried out at SCK CEN.

#### 2. Methods and Results

In this section, the atomistic simulation details and experimental procedures are described. All the atomistic simulations in this study were performed using the LAMMPS code [4] using the moment tensor potential (MTP) developed in our previous study [2] for bodycentered cubic (bcc) Fe and liquid Pb.

# 2.1 Semi-grand canonical Monte-Carlo ensemble simulation

The semi-grand canonical ensemble samples the possible states of a mixture in thermodynamic equilibrium with a reservoir at constant temperature and chemical potential for each species. This ensemble gives a set of configurations with varying compositions, the

ensemble average of which converges to the energetically favorable composition, as constrained by the reservoir. Along with the Monte-Carlo algorithm, trial moves are made to vary the composition by randomly selecting a particle and swapping its species. For a binary mixture of total N atoms at temperature T with the given chemical potential difference between the two species  $\Delta\mu$ , the acceptance probability of these trial moves is

$$p = \min\left(1, \exp\left[-\frac{\Delta U + \Delta \mu N \Delta c}{k_B T}\right]\right), \tag{1}$$

where  $\Delta U$  and  $\Delta c$  are the calculated changes in energy and concentration, respectively.

The chemical potentials were calculated by thermodynamic integration (TI), in reference to a system with its absolute free energy known priori, which is written as

$$F_{\rm Int} = F_{\rm Ref} + \int_0^1 \left\langle \frac{\partial U(\lambda)}{\partial \lambda} \right\rangle_{\lambda} d\lambda, \qquad (2)$$

where  $\lambda$  is the coupling parameter that drives the system from the reference system to the system of interest. We chose the Einstein crystal (EC) and Uhlenbeck-Ford (UF) fluid [5] as the reference systems for bcc Fe and liquid Pb, respectively.

Using the chemical potential calculated at 1000 K, we performed the SGCMC simulations for solubility calculation with initially 32000 Pb atoms at 1000 K with 20 samples. This high temperature was considered with two reasons: to accelerate the simulation to reach a visibly high concentration with an affordable system size and to supplement missing measurement data at high temperature where wüstites (FeO) are expected to form in contrast to that magnetites (Fe<sub>3</sub>O<sub>4</sub>) form at normal temperature ranges, according to the Ellingham diagram of the Fe oxides in liquid Pb. Figure 1 shows the averaged Fe concentration in liquid Pb as a function of time. The solubility limit was estimated by averaging over the last 0.01 ns.

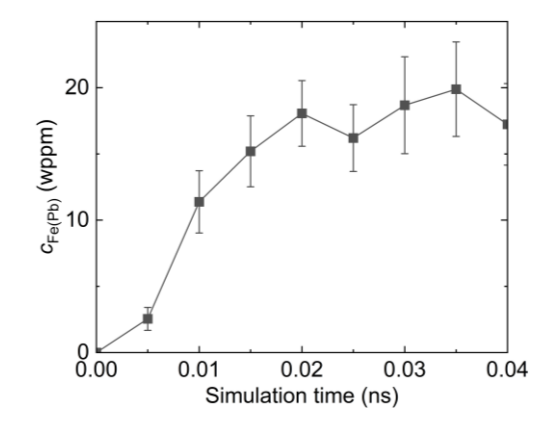


Figure 1. Average Fe concentration in liquid Pb in wppm as a function of simulation time in SGCMC simulations at 1000 K.

#### 2.2 Electrochemical measurement

The concept of this in-situ electrochemical measurement method [1] is that the elemental solubility can be derived from the solubility product of the oxide forming. The reaction equation for the formation of Fe oxide and its solubility product at temperature above 600°C is given by

$$FeO_{(s)} \rightleftharpoons Fe_{(Pb)} + [O]_{(Pb)},$$
 (3)

$$K_{\rm SP} = c_{\rm Fe(Pb)} c_{\rm O(Pb)}, \tag{4}$$

where  $c_{\rm Fe(Pb)}$  and  $c_{\rm O(Pb)}$  are the Fe and O concentration in liquid Pb, respectively. At saturation of Fe, the solubility is written as follows.

$$S_{\text{Fe(Pb)}} = \frac{\kappa_{\text{SP}}}{c_{\text{O(Pb)},\text{Fe(Pb)} \leftrightarrow \text{Fe(s)}}} \tag{5}$$

where  $c_{O(Pb),Fe(Pb)\leftrightarrow Fe(s)}$  is the O concentration at Fe saturation. The solubility product can be derived by fitting the measured time derivative of O concentration during pumping into the following model equation,

$$\frac{dc_{0}(t)}{dt} = \frac{r_{0}(t)}{1 + \frac{M_{0}}{M_{Fe}} K_{SP} c_{0}^{-2}(t)}$$
 (6)

where  $r_O(t)$  is the oxygen pumping rate in wt%/s, and  $M_O$  and  $M_{Fe}$  are the molar masses of O and Fe, respectively. The O concentration at saturation can be derived in terms of thermochemical data as

$$c_{\text{O(Pb),Fe(Pb)} \leftrightarrow \text{Fe(s)}} = \frac{e^{\left(\frac{\Delta_f G_{\text{FeO}}}{RT}\right)}}{k_O}, \tag{7}$$

where  $\Delta_f G_{\text{FeO}}^{\circ}$  is the Gibbs free energy of formation of FeO [6], and  $k_0$  is the Sieverts' constant of O in liquid Pb [7].

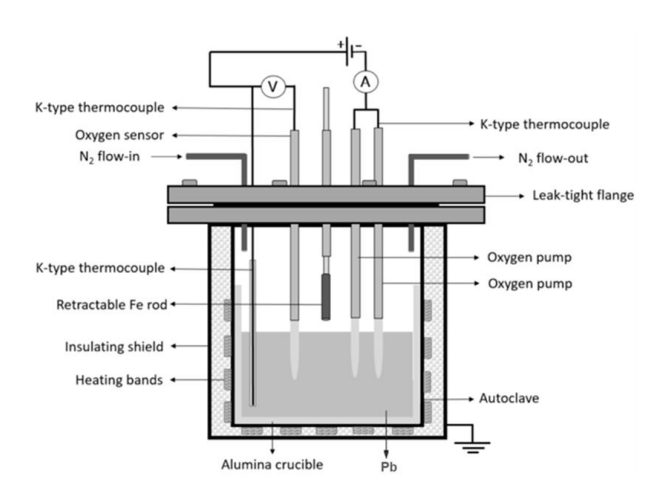


Figure 2. Schematic description of the experimental setup for solubility measurement [1].

Figure 2 describes the experimental setup for solubility measurement. A pure Pb (99.99%, 1532 g) was melted in the crucible. A high purity Fe rod (99.97%) was inserted into the clave and left until Fe to be saturated in liquid Pb. Oxygen pumping was performed until the O concentration reached a value corresponding to the Fe concentration was approximately 20% of the expected solubility as recommended in [1]. The oxygen leak rate was measured before pumping and added to the pumping rate, assuming a constant value in wt%/s.

Figure 3 shows an example of the evolution of O concentration in liquid Pb measured during the whole procedure. The O concentration at Fe saturation was in good agreement with the estimate from equation (7) referring to the available thermochemical data [6,7].

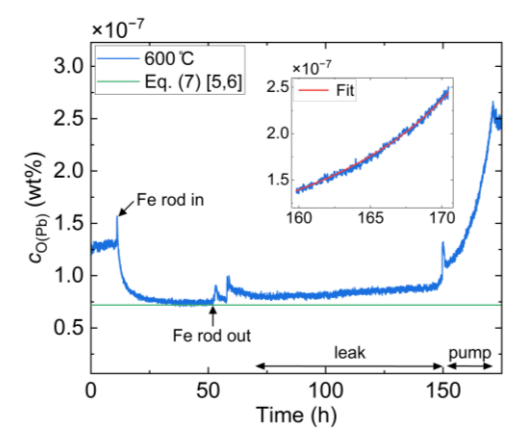


Figure 3. Evolution of O concentration in liquid Pb in wt% measured at 600°C with the insert of the fitting curve during pumping.

### 2.3 Fe solubility in liquid Pb

Figure 4 shows the calculated and measured Fe solubility in liquid Pb in comparison with available data [2,8–10]. Compared to our previous result [2], the SGCMC result is 2-3 times higher. This accuracy is

satisfactory enough considering the saved computational cost although the DCM is supposed to be more intuitive and accurate. As the error sources of this SGCMC method, we can consider the followings. First, there might be some errors in the absolute free energy formulation of the reference system for the chemical potential calculation. Depending on the choice of the reference system, the chemical potentials can be different. For liquid Pb, we tested the Lennard-Jones (LJ) fluid as well, however we found the instability of the LJ fluid to describe liquid Pb at relatively lower temperatures near the melting point of Pb. Second, the difference in the atomic sizes between two species can cause local residual stresses right after a species was swapped to another one, which makes the system pressure slightly away from zero although the equilibrium composition should not be largely affected by this factor.

On the other hand, according to the Ellingham diagram of the Fe oxides in liquid Pb, the FeO oxidation appears to be thermodynamically more stable than the  $Fe_3O_4$  oxidation at temperatures above  $\sim 600^{\circ}C$ . In Figure 4, there seems to be no noticeable transition in the solubility near  $600^{\circ}C$ , indicating that this electrochemical measurement based on oxide formation works regardless of the type of oxide.

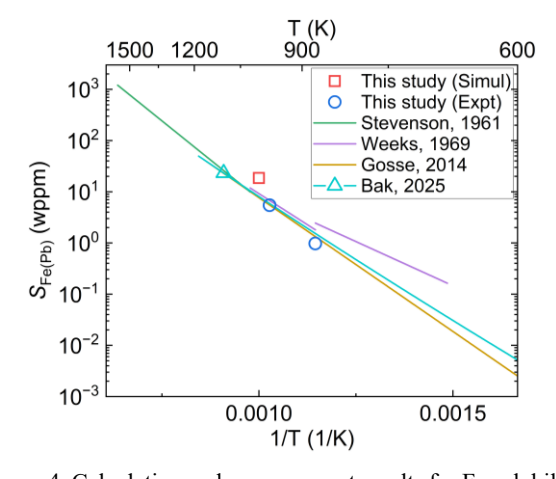


Figure 4. Calculation and measurement results for Fe solubility in liquid Pb in comparison with available data.

#### 3. Conclusions

As one of the key properties related to steel corrosion by heavy liquid metals, the Fe solubility in liquid Pb was calculated by the SGCMC ensemble method. The calculation results were validated by the electrochemical measurements. The SGCMC method showed satisfactory accuracy in agreement with the experiments and previous simulations.

Thanks to the simplicity of bulk system of the SGCMC method, escaping from the complicated interface system of the DCM, the calculation cost is greatly reduced during the solubility calculation. It will save the calculation cost in the potential model construction phase as well if we construct a potential model from the beginning, although we used the

previously developed MTP in this study. The Monte-Carlo swapping also contributes to accelerate the simulations to reach the equilibrium quickly.

This study highlights that atomistic simulations can be an alternative to experiments for solubility of elemental impurities in liquid metals with affordable computational costs. A practical limitation of the SGCMC is that its parallel algorithm is optimized only for the embedded atom method (EAM) potential in the current LAMMPS implementation, which needs extension to the recent machine learning potentials to improve the accuracy.

#### **ACKNOWLEDGEMENTS**

This work was supported by the Korea Institute of Energy Technology Evaluation and Planning(KETEP) and the Ministry of Trade, Industry & Energy(MOTIE) of the Republic of Korea (No. RS-2024-00487321).

#### REFERENCES

- [1] G. Gregori, A. Aerts, K. Gladinez, K. Rosseel, T. Doneux, J. Lim, Electrochemical measurement of solubility product of metal oxides in liquid metals by coulometric titration of oxygen, Electrochim Acta 432 (2022).
- [2] S. Bak, T. Oda, Generation and correction of machine learning interatomic potential for simulation of liquid metal corrosion with near experimental accuracy: A study for iron corrosion in liquid lead, Corros Sci 242 (2025).
- [3] B. Sadigh, P. Erhart, A. Stukowski, A. Caro, E. Martinez, L. Zepeda-Ruiz, Scalable parallel Monte Carlo algorithm for atomistic simulations of precipitation in alloys, Phys Rev B Condens Matter Mater Phys 85 (2012).
- [4] S. Plimpton, Fast parallel algorithms for short-range molecular dynamics, J Comput Phys 117 (1995).
- [5] R. Paula Leite, R. Freitas, R. Azevedo, M. De Koning, The Uhlenbeck-Ford model: Exact virial coefficients and application as a reference system in fluid-phase free-energy calculations, Journal of Chemical Physics 145 (2016).
- [6] HSC Chemistry, Version 9.9.0.1, Chemical Reaction and Equilibrium Software, Outotec. (n.d.).
- [7] J. Lim, K. Gladinez, A. Marino, K. Rosseel, A. Aerts, Solubility of oxygen and metastable limit for PbO nucleation in liquid Pb, JOM 73 (2021) 4023–4029.
- [8] D.A. Stevenson, J. Wulff, Liquid-solid phase distribution studies in the systems iron-lead, cobalt-lead, chromium-tin, and nickel-silver, Transactions of the Metallurgical Society of AIME 221 (1961) 271–275.
- [9] J.R. Weeks, A.J. Romano, Liquidus curves and corrosion of Fe, Ti, Zr, and Cu in liquid Bi-Pb alloys, 25 (1969) 131–136.
- [10] S. Gossé, Thermodynamic assessment of solubility and activity of iron, chromium, and nickel in lead bismuth eutectic, Journal of Nuclear Materials 449 (2014) 122–131.